IEEE Transactions on Nuclear Science NS-41, pp. 1441–1445 (1994) *LBL–34873*

DESIGN STUDIES FOR A PET DETECTOR MODULE USING A PIN PHOTODIODE TO MEASURE DEPTH OF INTERACTION*

W. W. Moses and S. E. Derenzo
Lawrence Berkeley Laboratory, University of California, Berkeley, CA 94720

Abstract

We present design studies of a multi-layer PET detector module that uses an 8x8 array of 3 mm square PIN photodiodes to both identify the crystal of interaction and measure the depth of interaction. Each photodiode is coupled to one end of a 3x3x30 mm BGO crystal, with the opposite ends of 64 such crystals attached to a single 1" square photomultiplier tube that provides a timing signal and energy discrimination. Each BGO crystal is coated with a lossy reflector, so the ratio of light detected in the photodiode and photomultiplier tube depends on the interaction depth in the crystal, and is used to determine this depth of interaction on an event by event basis.

A test module with one 3x3x30 mm BGO crystal, one 3 mm square PIN photodiode, and one photomultiplier tube is operated at –20˚ C with an amplifier peaking time of 4 μs, and a depth of interaction resolution of 5 to 8 mm fwhm measured. Simulations predict that this virtually eliminates radial elongation in a 60 cm diameter BGO tomograph. The photodiode signal corresponding to 511 keV energy deposit varies linearly with excitation position, ranging from 1250 electrons (e^-) at the end closest to the photodiode to 520 e^- at the opposite end. The electronic noise is a position independent 330 e^- fwhm, so the signal to noise ratio is sufficient to reliably identify the crystal of interaction in a 64 element module.

1. INTRODUCTION

The radial elongation artifact in PET (caused by annihilation photons penetrating into adjacent crystals in the tomograph ring before interacting and being detected) has long been recognized as an obstacle to high resolution PET. For 20 cm diameter objects this artifact is barely noticeable in whole body PET cameras (ring diameter ≥80 cm), it causes significant degradation towards the edge of the field of view in cerebral cameras (ring diameter 50–80 cm) and dominates the resolution in small animal PET cameras (ring diameter <50 cm).

The method for reducing or eliminating this artifact without reducing sensitivity is also well understood – the detector module must both identify the crystal that the 511 keV photon interacts in and measure the distance that it penetrates into the crystal before interacting (*i.e.* the depth of interaction). Numerous strategies have been proposed for constructing detector modules that measure the depth of interaction [1–9], but all have proved impractical to implement or provided insufficient depth of interaction measurement resolution, and so none have been incorporated into a full PET camera.

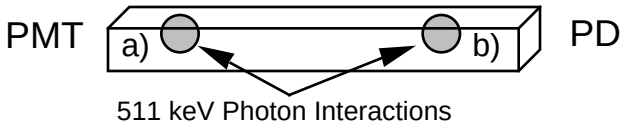

Figure 1: Depth of interaction measurement method. The scintillator crystal is coupled to a photomultiplier (PMT) and a photodiode (PD) and the other faces coated with a "lossy" reflector. Interactions near the PMT, as in a), result in a large PMT signal and a small PD signal. Interactions near the PD, as in b), result in a small PMT signal and a large PD signal.

In this paper we propose a PET detector module that measures the depth of interaction. A simple, single element detector module is constructed and characterized for both its depth of interaction measurement resolution and the signal to noise ratio observed when 511 keV photons interact in the module. Monte Carlo simulations are used to extrapolate the test module results to the performance of a PET camera based on the proposed module.

2. BACKGROUND

The method for determining the depth of interaction is shown schematically in Figure 1. The module is composed of 3x3x30 mm BGO crystals that are coupled on one 3x3 mm face to a silicon photodiode and on the opposing face to a photomultiplier tube. The 3x30 mm faces are coated with a "lossy" reflector so that the magnitude of the signal observed in the photodiode and the photomultiplier tube depends on the depth of the 511 keV photon interaction in the scintillator crystal. The ratio of these two signals can then be used to determine the depth of interaction on an event by event basis.

These elements can be combined as in Figure 2 to form a PET detector module consisting of an 8 by 8 array of optically isolated 3 mm square by 30 mm deep BGO crystals, each coupled on one 3x3 mm face to a silicon photodiode and on the other 3x3 mm face to a one inch square photomultiplier tube. The photomultiplier tube provides a timing pulse and initial energy discrimination, the photodiodes identify the crystal of interaction, and the combination measure the depth of interaction. The photodiodes are read out with four 16-channel, low noise charge sensitive amplifier integrated circuits [10] (not shown in Figure 2) mounted on the back (non-photosensitive) side of the photodiode array.

*** This work was supported in part by the U.S. Department of Energy under Contract No. DE-AC03-76SF00098, and in part by Public Health Service Grant Nos. P01 25840, R01 CA48002, and R01 NS29655.**

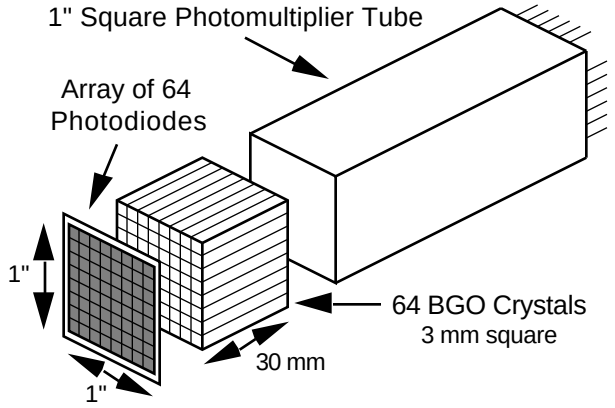

Figure 2: Exploded view of the proposed PET module. Each BGO crystal is attached to a photomultiplier tube, which provides a timing pulse and initial energy discrimination, and to a photodiode, which identifies the crystal of interaction. The signals are combined to measure the depth of interaction.

3. SINGLE DETECTOR ELEMENT MODULE PERFORMANCE

To test this detector concept, we constructed a module consisting of a single 3x3x30 mm BGO crystal, with one end coupled to a 3 mm square PIN photodiode and the opposite end coupled to a 3/8 inch square photomultiplier tube. The PIN photodiode is a Hamamatsu S-2506 (2.77 mm square active area, 100 μm depletion thickness) mounted in a special package to allow close coupling to the scintillator crystal. A "lossy" reflector is made by sanding the BGO crystal before applying a white refelective coating. For this and all subsequent measurements, the photodiode is biased with +30 V and the assembly cooled to –20˚ C. Under these operating conditions, the capacitance is 9 pF and the dark current is <1 pA.

The assembly is cooled in order to increase the light output from BGO. Operation at –20˚ C increases the light output by a factor of 1.7 compared to room temperature (+25˚ C) operation, but the decay time increases from its room temperature value of 300 ns to 675 ns [11]. An amplifier with a 4 μs shaping time processes the photodiode signal, and a calibrated test pulse is used to determine the noise, which is 330 electrons (e^-) fwhm.

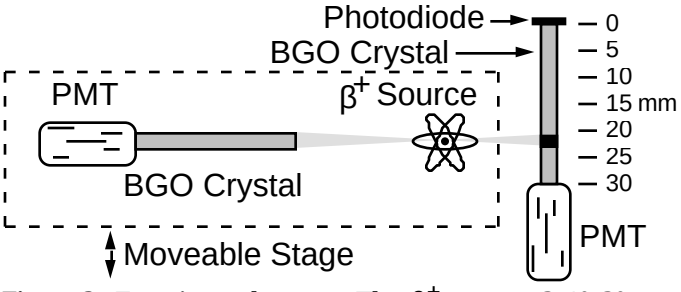

Figure 3: Experimental set-up. The β^+ source, 3x10x30 mm BGO crystal, and photomultiplier tube provide an electronically collimated beam (2.5 mm fwhm) whose position is adjusted by moving the entire assembly.

This test module is illuminated with an electronically collimated beam of annihilation photons from a ^{68}Ge source, as shown in Figure 3. The position of the beam is varied by moving the entire collimation apparatus, allowing a 2.5 mm fwhm portion of the test module to be excited at an arbitrary depth of interaction. The depth coordinate system is chosen such that 0 mm corresponds to the end of the BGO crystal closest to the photodiode and 30 mm is the end closest to the photomultiplier tube.

Whenever a coincidence between photomultiplier tubes occurs, the signals in the test module photodiode and photomultiplier tube are simultaneously digitized and read into a computer. Figures 4a and 4b plot the pulse height spectrum observed in the photodiode and photomultiplier tube respectively at three excitation depths. A clear 511 keV photopeak is observed at all excitation depths in both the photomultiplier tube and the photodiode. The position of the photopeaks is depth dependent, with excitation at 2 mm depth (*i.e.* near the photodiode) resulting in low photomultiplier and high photodiode pulse heights and excitation at 28 mm depth (*i.e.* near the photomultiplier tube) resulting in high photomultiplier and low photodiode pulse heights.

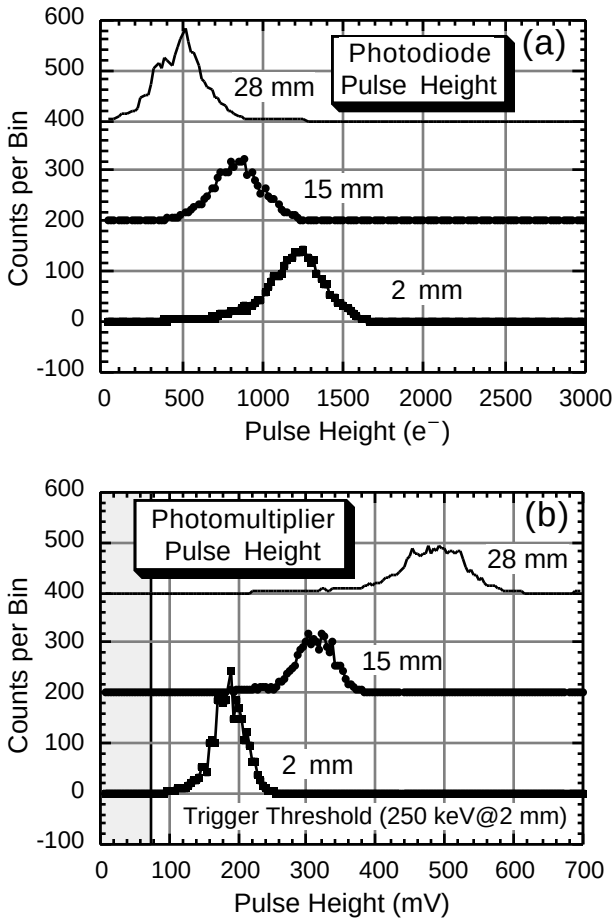

Figure 4: Pulse height plots as a function of excitation position, showing the 511 keV photon peak for both (a) the photodiode and (b) the photomultiplier tube.

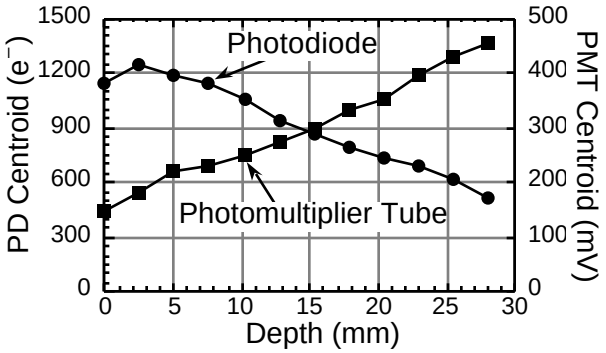

Figure 5: Position of the centroid of the 511 keV photon peak as a function of excitation position, for both the photodiode and the photomultiplier tube. Note that both are linear functions of position, and have different measurement units.

In a PET imaging situation, the depth of interaction is not known when the photomultiplier tube triggers, so a fixed discriminator voltage must be used in the trigger. The conversion from voltage to energy deposit depends on the depth of interaction, so the energy equivalent trigger threshold is also position dependent. This situation is mimicked in these tests by using a fixed discriminator voltage of 75 mV, which corresponds to 250 keV energy deposit when the test module is excited at 2 mm depth and 85 keV when excited at 28 mm depth. After readout, the amplitudes of the photodiode and photomultiplier tube signals can be converted to energy as described below and an energy threshold applied to the summed signals. This is done for all data presented in this paper (including Figure 4) with a 250 keV threshold.

The centroid of the 511 keV photopeak in each detector is computed as a function of excitation depth and plotted in Figure 5. The dependence of the photodiode and photomultiplier tube centroids on position is approximately linear but have different measurement units. To compare the outputs of the two sensors, one of them (the photomultiplier tube was chosen arbitrarily) must be rescaled. A simple linear plus offset transformation (*i.e.* $y = mx + b$) is applied, with the constants *m* and *b* chosen so the position of the 511 keV photopeak at 2 mm (as observed by the photomultiplier tube) is equal to the position of the photopeak at 28 mm (as observed by the photodiode) and vice versa. This results in an equal energy scale, allowing the energy deposit observed by both photodetectors to be directly compared.

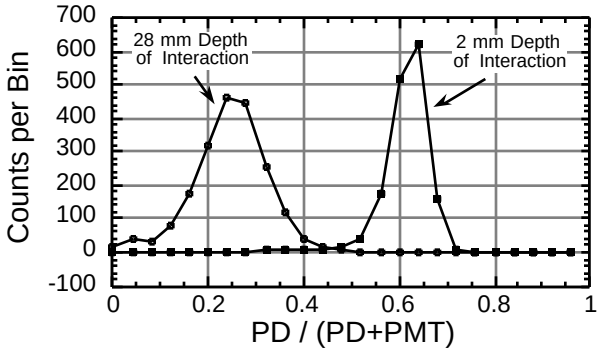

Figure 6: Distribution of the position estimator PD / (PD+PMT) with the test module excited at fixed depths of interaction of 2 and 28 mm.

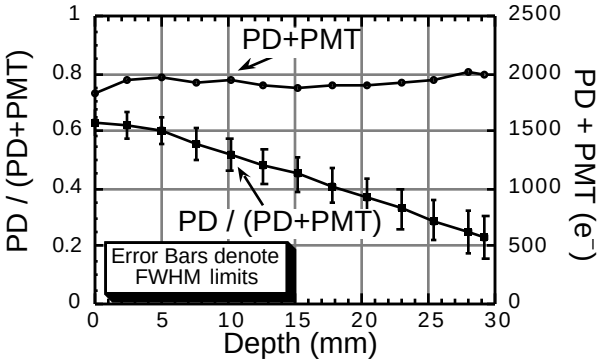

Figure 7: Value of the position estimator PD / (PD+PMT) and the sum signal PD+PMT versus depth of interaction.

The position of interaction is measured on an event by event basis by computing a position estimator. This estimator is defined as the fraction of the summed output from two photodetectors that is observed by the photodiode, or PD / (PD+PMT), where PD is the pulse height observed by the photodiode and PMT is the rescaled pulse height observed by the photomultiplier tube. A plot of this ratio is shown in Figure 6 with the test module excited at interaction depths of 2 and 28 mm.

The collimated excitation beam is scanned along the test module, and at each depth of interaction the centroid and fwhm of the depth estimator PD / (PD+PMT) are computed, as is the position of the 511 keV photopeak in the sum signal PD+PMT. Figure 7 plots these measurements as a function of depth of interaction, with the fwhm of the depth estimator represented as error bars on the estimator. While the sum signal PD+PMT is essentially independent of the depth of interaction, the centroid of the PD / (PD+PMT) estimator is linearly dependent on depth, and the fwhm of this estimator increases with increasing depth (since the noise in the photodiode is constant but the signal decreases with increasing depth). Dividing the fwhm of the depth estimator by the slope yields the depth of interaction measurement resolution, which varies from 5 mm fwhm at a depth of 2 mm to 8 mm fwhm at a depth of 30 mm.

4. Monte Carlo Prediction of Module Performance

The performance of a single detector element must be extrapolated using a Monte Carlo simulation to predict the performance of a multi-element module or a complete PET camera. Two important questions that can be addressed through Monte Carlo simulation: 1) what fraction of events will be mis-identified because of noise fluc-

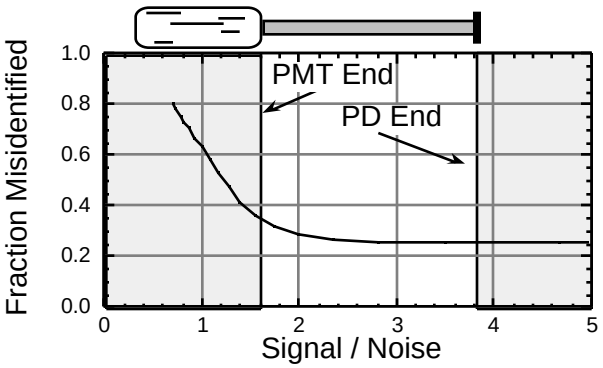

Figure 8: Fraction of incorrectly identified events as a function of the signal to noise ratio in the photodiode.

tuations in the photodiode array and 2) how will 5–8 mm depth of interaction measurement resolution affect the reconstructed resolution of a PET camera?

The dependence on the fraction of mis-identified events on the 511 keV signal to noise ratio in the photodiode in a 64 element detector has been reported previously [12] and the results are reproduced in Figure 8. For small signal to noise ratios, the mis-identification fraction approaches unity, while for high ratios it approaches 25%. This 25% asymptote is due to primary 511 keV photons that Compton scatter in the detector module and are subsequently absorbed in the same module, with the secondary photon having greater energy than the primary energy deposit.

Since the signal to noise ratio in the proposed module depends on the depth of interaction, the fraction of mis-identified events is also depth dependent, but lies within the unshaded regions of Figure 8. Interactions that occur near the photodiode end of the module (which most do, due to the 1.2 cm exponential attenuation length of BGO) have a fraction of mis-identified events that is close to its asymptotic value of 25%, while the fraction rises to 35% for interactions at the photomultiplier tube end. In short, the noise in the photodiode signal will have minimal effect on the mis-identification fraction.

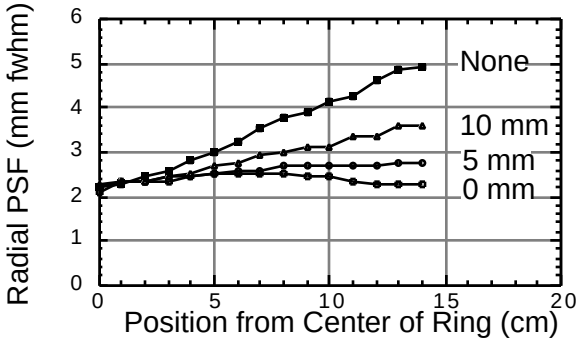

Figure 9: Radial component of the reconstructed point spread function for depth of interaction measurement resolutions of 0, 5, and 10 mm fwhm, and without depth of interaction measurement. The PET camera simulated had a 60 cm ring diameter and 3 mm BGO crystals.

The predicted dependence of the reconstructed point spread function (PSF) on the depth of interaction measurement resolution has been previously reported for a PET camera with 60 cm ring diameter and 3 mm wide BGO crystals [13], and the results shown in Figure 9. This figure shows that without depth of interaction measurement, the radial component of the PSF of 2.4 mm fwhm obtained near the center of the tomograph increases to 4.1 mm at a radius of 10 cm. With the depth of interaction measurement resolution obtained by this test module (between 5 and 8 mm), the radial component of the PSF at 10 cm radius should be reduced to 3 mm or less. The effect of radial elongation on tomographs with the same crystal size but different ring diameters can be estimated by scaling the x-axis of Figure 9 by the ratio of the ring diameters. Therefore, the PSF at 10 cm radius in a 40 cm diameter ring will be similar to the PSF at 15 cm radius in a 60 cm diameter ring.

5. POTENTIAL FOR IMPLEMENTATION

One possible implementation of a PET camera constructed from these detector modules is a high resolution, high sensitivity cerebral scanner. The detector ring diameter would be as small as possible to reduce the resolution degradation from annihilation photon acollinearity, and the depth of interaction measurement would virtually eliminate the degradation from radial elongation. If the camera were constructed without septa, it could be as small as 40 cm diameter and still have space for an orbiting transmission source. While a multi-ring, septaless design would be vulnerable to annihilation photons scattered in the patient, it would ensure the possibility of high sensitivity 3-D data collection, although septaless 2-D acquisition could be used to reduce the data set size. The small ring diameter would also reduce the cost of the scanner significantly.

Several concerns must be addressed before a PET camera is constructed from these detector modules. One concern is the feasibility of operating the tomograph gantry at –20˚ C. While a cooling system and thermal insulation are easily incorporated, servicing the camera and preventing condensation would be difficult. This problem could be overcome by using a scintillator with higher light output at room temperature, such as LSO [14], but LSO is currently costly and not available in the quantities necessary for a tomograph.

Another concern is that the dependence of the photodiode / photomultiplier tube light ratio versus depth of interaction must be known for each crystal in the tomograph. Even a small tomograph would have thousands of individual crystals, and so these crystals (and their lossy coating) must be manufactured with nearly identical optical properties. The remaining non-uniformities must be removed by calibration, which is difficult because one cannot calibrate by forcing annihilation photons to interact at a specific depth of interaction. However, this

calibration could be performed using a line source at the center of the ring and adjusting the calibration parameters to achieve the 1.2 cm attenuation length of BGO.

A final concern is the cost of the system. Individual 3x3 mm silicon photodiodes are relatively inexpensive (less than $1 each), but an 8x8 array of these photodiodes would probably cost over $100 due to the lower yield. The parts cost for a conventional PET detector module is approximately $600 per square inch ($400 for BGO and $200 for photomultiplier tubes), so adding the photodiode array would increase the cost of each detector module by about 20%. However, the smaller ring diameter uses 50% fewer detector modules than a conventional whole body camera, and so the net parts cost of the PET camera described above would be reduced.

6. CONCLUSIONS

A PET detector module that uses an array of silicon photodiodes to both identify the crystal of interaction and measure the depth of interaction has been proposed. In order to obtain sufficient signal to noise ratio in the photodiode, the light output of the BGO scintillator crystals was increased by cooling the detector module to –20° C. A single element test module was constructed, and the average signal observed by the photodiode and photomultiplier tube varied linearly with the depth of interaction, ranging from 1250 e^- to 520 e^- per 511 keV photon interaction for the photodiode and from 150 mV to 450 mV for the photomultiplier tube. The electronic noise in the photodiode was a depth independent 330 e^- fwhm. The ratio of the signals observed by the photodiode and the photomultiplier tube was used to measure the depth of interaction on an event by event basis. The accuracy of this depth measurement ranged from 5 mm fwhm at the photodiode end of the module (*i.e.* the patient end) to 8 mm at the photomultiplier tube end.

Monte Carlo simulations were used to extrapolate the performance of the single element test module to a 64 element detector module and a complete PET camera. These simulations predict that misidentification of the crystal of interaction due to noise fluctuations in the photodiode will not be a significant problem, and that radial elongation would effectively be eliminated in a 60 cm diameter PET camera made with these modules. A high resolution, high sensitivity cerebral PET scanner based on these crystals was proposed, but the feasibility of –20° C gantry operation, manufacturing and calibration methods that maintain uniform dependence of the light ratio on depth for all crystals, and cost must all be studied before such a PET camera can be constructed.

ACKNOWLEDGMENTS

We thank Mr. T. Vuletich and Mr. M. Ho of Lawrence Berkeley Lab for invaluable technical support, and Dr. T. Budinger, Dr. R. Huesman, and Dr. R. Nutt of Lawrence Berkeley Lab and CTI, Inc. for useful discussions. This work was supported in part by the Director, Office of Energy Research, Office of Health and Environmental Research, Medical Applications and Biophysical Research Division of the U.S. Department of Energy under contract No. DE-AC03-76SF00098, in part by the National Institutes of Health, National Heart, Lung, and Blood Institute, National Cancer Institute, and National Institute of Neurological Disorders and Stroke under grants No. P01-HL25840, No. R01-CA48002, and No. R01-NS29655.

REFERENCES

[1] Del Guerra A, Perez-Mendez V, Schwartz G, et al. Design considerations for a high spatial resolution positron camera with dense drift space MWPC's. *IEEE Trans. Nucl. Sci.* **NS-30:** pp. 646–651, 1983.

[2] Wong HH. Designing a stratified detection system for PET cameras. *IEEE Trans. Nucl. Sci.* **NS-33:** pp. 591–596, 1986.

[3] Rogers JG, Saylor DP, Harrop R, et al. Design of an efficient position sensitive gamma ray detector for nuclear medicine. *Phys. Med. Biol.* **31:** pp. 1061–1090, 1986.

[4] Karp J and Daube-Witherspoon M. Depth-of-interaction determination in NaI(Tl) and BGO scintillation crystals using a temperature gradient. *Nucl. Instr. Meth.* **A-260:** pp. 509–517, 1987.

[5] Carrier C, Martel C, Schmitt D, et al. Design of a high resolution positron emission tomograph using solid state scintillation detectors. *IEEE Trans. Nucl. Sci.* **NS-35:** pp. 685–690, 1988.

[6] Shimizu K, Ohmura T, Watanabe M, et al. Development of a 3-D detector system for positron CT. *IEEE Trans. Nucl. Sci.* **NS-35:** pp. 717–720, 1988.

[7] Derenzo S, Moses W, Jackson H, et al. Initial characterization of a position-sensitive photodiode/BGO detector for PET. *IEEE Trans. Nucl. Sci.* **NS-36:** pp. 1084–1089, 1989.

[8] Yamashita Y, Watanabe M, Shimizu K, et al. High resolution block detectors for PET. *IEEE Trans. Nucl. Sci.* **NS-37:** pp. 589–593, 1990.

[9] Bartzakos P and Thompson CJ. A Depth-Encoded PET Detector. *IEEE Trans. Nucl. Sci.* **NS-38:** pp.732–738, 1991.

[10] Moses WW, Kipnis I and Ho MH. A 16-channel charge sensitive amplifier IC for a PIN photodiode array based PET detector module. *IEEE Trans. Nucl. Sci.* **NS-41:** (submitted for publication), 1994.

[11] Melcher CL, Schweitzer JS, Liberman A, et al. Temperature dependence of fluorescence decay time and emission spectrum of bismuth germanate. *IEEE Trans. Nucl. Sci.* **NS-32:** pp. 529-532, 1985.

[12] Moses WW, Derenzo SE, Nutt R, et al. Performance of a PET detector module utilizing an array of silicon photodiodes to identify the crystal of interaction. *IEEE Trans. Nucl. Sci.* **NS-40:** pp. 1036–1040, 1993.

[13] Moses WW, Huesman RH and Derenzo SE. A new algorithm for using depth-of-interaction measurement information in PET data acquisition. *J. Nucl. Med.* **32:** pp. 995, 1991.

[14] Melcher CL and Schweitzer JS. Cerium-doped lutetium orthosilicate: A fast, efficient new scintillator. *IEEE Trans. Nucl. Sci.* **NS-39:** pp. 502-504, 1992.